

Hierarchical assembly and the onset of banding in fibrous long spacing collagen revealed by atomic force microscopy

Jan K. Rainey, Chuck K. Wen, M. Cynthia Goh*

Department of Chemistry, University of Toronto, 80 St. George Street, Toronto, Ont., Canada M5S 3H6

Received 17 April 2002; received in revised form 22 October 2002; accepted 31 October 2002

Abstract

The mechanism of formation of fibrillar collagen with a banding periodicity much greater than the 67 nm of native collagen, i.e. the so-called fibrous long spacing (FLS) collagen, has been speculated upon, but has not been previously studied experimentally from a detailed structural perspective. *In vitro*, such fibrils, with banding periodicity of ~270 nm, may be produced by dialysis of an acidic solution of type I collagen and α_1 -acid glycoprotein against deionized water. FLS collagen assembly was investigated by visualization of assembly intermediates that were formed during the course of dialysis using atomic force microscopy. Below pH 4, thin, curly nonbanded fibrils were formed. When the dialysis solution reached ~pH 4, thin, filamentous structures that showed protrusions spaced at ~270 nm were seen. As the pH increased, these protofibrils appeared to associate loosely into larger fibrils with clear ~270 nm banding which increased in diameter and compactness, such that by ~pH 4.6, mature FLS collagen fibrils begin to be observed with increasing frequency. These results suggest that there are aspects of a stepwise process in the formation of FLS collagen, and that the banding pattern arises quite early and very specifically in this process. It is proposed that typical 4D-period staggered microfibril subunits assemble laterally with minimal stagger between adjacent fibrils. α_1 -Acid glycoprotein presumably promotes this otherwise abnormal lateral assembly over native-type self-assembly. Cocoon-like fibrils, which are hundreds of nanometers in diameter and 10–20 μ m in length, were found to coexist with mature FLS fibrils. © 2002 Elsevier Science B.V./International Society of Matrix Biology. All rights reserved.

Keywords: Self-assembly; Scanning probe microscopy; α_1 -Acid glycoprotein (orosomuroid); Type I collagen; pH dependence; Static light scattering; Tactoid

1. Introduction

The fibril forming collagens may produce a variety of constructs with different dimensions and ultrastructural morphologies both *in vivo* and *in vitro* (Eyden and Tzaphlidou, 2001; Ghadially, 1988; Kadler et al., 1996; Kuhn, 1982; Nimni, 1988). Preferential formation of such constructs may be induced *in vitro* by subjecting the collagen monomer to various solution conditions. The typical fibrillar form of collagen is termed native-type, and is characterized by the presence of banding with ~67 nm period that is clearly visible by transmission electron microscopy (TEM) or scanning electron

microscopy (Chapman et al., 1990; Ghadially, 1988) and atomic force microscopy (AFM, Baselt et al., 1993; Bowen et al., 2000; Gale et al., 1995; Revenko et al., 1994). Collagen fibrils with periodicity clearly greater than this have been observed both *in vivo* and *in vitro*, and are generally classified as fibrous long spacing (FLS) collagen (Eyden and Tzaphlidou, 2001; Ghadially, 1988).

Typical studies of the morphologies of collagenous structures have been by TEM, in which image contrast is caused by the relative ability of regions of the sample to scatter or transmit electrons. Sample staining with heavy, electron scattering elements is often carried out in order to enhance the contrast within organic samples, such as collagen. Staining patterns exhibited by various collagen constructs have been instrumental in the interpretation of the supramolecular architecture of the constructs in question (Chapman et al., 1990). In the case of AFM studies, beyond the drying on a flat imaging

Abbreviations: AFM, atomic force microscopy; EM, electron microscopy; FLS, fibrous long spacing; TEM, transmission electron microscopy.

*Corresponding author. Tel.: +1-416-978-6254; fax: +1-416-978-4526.

E-mail address: cgoh@alchemy.chem.utoronto.ca (M.C. Goh).

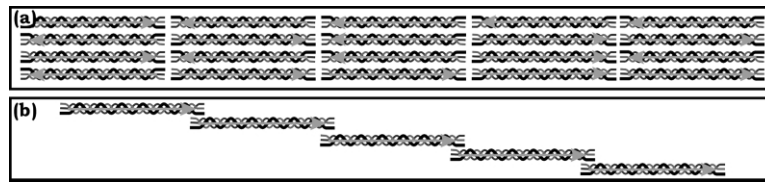


Fig. 1. Schematic demonstrating the proposed packing of collagen monomer in FLS collagen with 250–270 nm banding (Gross et al., 1954) arising from a 0D-staggered array (a) of end-on-end collagen monomers. For comparison, a pentamer of 4D-staggered monomers is illustrated schematically in (b). Note that type I collagen has a length of 280–300 nm (Nimni, 1988).

substrate also necessary in TEM, no sample treatment is needed. Instead, image contrast is based upon the interaction forces between a nanometer-sized probe and the sample surface. This provides, in the simplest and most frequently employed instance, a topographical image of the sample, possibly to sub-angstrom resolution (Bowen et al., 2000; Jandt et al., 2000; Kiselyova and Yaminsky, 1999). The technique of AFM readily allows itself to the examination of large numbers of samples with varying properties, permitting routine observation of the morphology and the assembly stages of fibrillar biomacromolecules, and has been applied to the study of collagen structure by various groups (Baselt et al., 1993; Fujita et al., 1997; Gale et al., 1995; Paige and Goh, 2001; Paige et al., 1998; Revenko et al., 1994). In vitro, the formation of FLS collagen may be readily induced in mixtures of collagen and α_1 -acid glycoprotein through the gradual increase of the pH from acidic to neutral (Highberger et al., 1950, 1951). The morphology of FLS collagen produced with α_1 -acid glycoprotein is highly reproducible, with a banding periodicity on the order of 250–270 nm demonstrated by both TEM (Gross et al., 1952, 1954; Highberger et al., 1950, 1951; Schmitt et al., 1953) and AFM (Paige et al., 1998, 2001). The structures of the final fibrillar forms of FLS collagen, formed both with α_1 -acid glycoprotein and with glycosaminoglycans such as chondroitin sulfate, have been the subject of several intensive studies (Chapman and Armitage, 1972; Franzblau et al., 1976; Gross et al., 1952, 1954; Highberger et al., 1950, 1951; Lin and Goh, 2002a,b; Lowther and Natarajan, 1972; Paige et al., 1998, 2001; Schmitt et al., 1953) and potential intermediate structures from FLS collagen assembly were reported by Gross et al. (1954). However, the structural and morphological features of the FLS collagen assembly pathway in vitro have never before been studied in detail.

Franzblau et al. (1976) carried out an extensive investigation of the interaction between α_1 -acid glycoprotein and collagen. Three major conclusions were reached in this study. First, it was determined that an increase in viscosity by $\sim 60\%$ is required in order to observe the long spacing morphology. Second, the removal of anionic sialyl groups from α_1 -acid glycoprotein prevents the formation of FLS collagen. Finally, the

approximate composition by mass of the final FLS collagen fibrils is 45–55% α_1 -acid glycoprotein. Each of these conclusions will be considered with respect to our results.

It has been proposed that the banding pattern in FLS collagen is due to collagen monomers aligned end-on-end with non-specific orientation (Franzblau et al., 1976; Gross et al., 1954), giving rise to a spacing with approximately the length of the monomer. The interpretation of monomer packing in this model was that no overlap was taking place between subsequent monomers lengthwise or laterally, leading to the later adoption of a ‘0D-period stagger’ being proposed for the FLS collagen fibril. The D here refers to the standard ~ 67 nm periodicity in native-type collagen (e.g. Kadler et al., 1996). (Note that the monomer length is ~ 280 – 300 nm (Nimni, 1988), as compared with the 250–270 nm banding that is observed by electron microscopy (EM) or AFM.) This discrepancy in length scale was addressed by the inclusion of an overlap in the FLS collagen model by various workers (reviewed in Doyle et al., 1975). A schematic of the proposed end-on-end packing of collagen monomers in FLS fibrils with 0D-stagger is given alongside a 4D-staggered pentamer, for comparison, in Fig. 1. Neither the 0D-stagger model or the later proposed models incorporating a stagger explicitly account for the necessity of α_1 -acid glycoprotein or for its inclusion in the FLS collagen fibril.

Previous AFM studies conducted in our group (Paige et al., 1998, 2001) showed an intricate surface ultrastructure of aligned protofibrillar units, with no evidence of individual monomer units, implying that the formation of protofibrils is a likely intermediate step. In TEM images, collagen fibrils display an alternating series of dark and light regions at the banding periodicity, where the dark regions are those that scatter electrons more readily. A direct correlation between TEM and AFM imaging of exactly the same fibrils with and without negative staining showed that these dark bands in TEM images correspond exactly to protrusions in the AFM images (Lin and Goh, 2002a,b). How these banding patterns arise has yet to be determined.

In this work, we address the fibrillogenesis pathway of FLS collagen assembled in vitro with α_1 -acid glycoprotein by direct visualization of assembly structures

using the AFM together with light scattering measurements. These experiments follow the approaches used in earlier studies of native-type collagen assembly using EM (Cox et al., 1967; Gelman et al., 1979; Holmes et al., 2001; Na et al., 1986; Trelstad et al., 1976; Vanamee and Porter, 1951; Wood and Keech, 1960) and AFM (Gale et al., 1995; Goh et al., 1997), where the presence of intermediate structures were demonstrated by sampling the assembly cocktail at various stages during fibrillogenesis. Two very different mechanisms for native collagen fibrillogenesis have been proposed: a simple nucleation and growth mechanism (developed in detail in Comper and Veis, 1977a,b) and a multistep hierarchical mechanism (reviewed in Trelstad, 1982). One complication in these studies arise from observation of different intermediates, depending upon the nature of the collagen starting material (reviewed in Holmes et al., 2001). Further AFM studies on assembly of collagenous structures have been carried out by correlation of the fibril diameter with growth in native-type fibrils (Christiansen et al., 2000), and by comparing the diameters of segmental long spacing collagen crystallites to their morphologies (Paige and Goh, 2001). While native-type collagen assembly has been studied by many techniques, FLS collagen assembly has not received equivalent attention.

Considering the drastic morphological and dimensional differences between FLS and native collagen fibrils, an understanding of the FLS collagen assembly process seems a crucial piece in the overall mosaic of collagenous construction. The observation *in vivo* of a variety of FLS type collagens, typically in pathological tissues (Eyden and Tzaphlidou, 2001; Ghadially, 1988), demonstrates the importance of understanding collagen fibrillogenesis beyond native-type collagen. The *in vitro* formation of FLS collagen with α_1 -acid glycoprotein provides an excellent starting point for such study, since it leads to fibrils with highly reproducible morphology (Gross et al., 1954; Highberger et al., 1951; Paige et al., 1998, 2001). In this investigation we observe hierarchical features in the FLS collagen fibrillogenesis pathway, analogous to those in native-type collagen. We also show for the first time the onset of protrusions, which, later in the fibrillogenesis, result in the characteristic FLS collagen banding pattern.

2. Results and discussion

We have produced FLS collagen fibrils previously by dialyzing acidic solutions of collagen and α_1 -acid glycoprotein against deionized water for ~ 17 h (Paige et al., 1998, 2001). Note that this is somewhat modified from the original methods of Highberger et al. (1950, 1951) where tap water and, later, distilled water were employed. In our previous work, an assembly mechanism was inferred from the ultrastructure of the mature FLS fibrils (Paige et al., 1998). In this paper we seek

to investigate the assembly pathway by examination of the self-assembly mixture during the time course of the dialysis. This was done by taking aliquots of the fibrillogenesis precipitating solution as a function of time, and subjecting each to light scattering and pH measurements, and to AFM imaging.

2.1. Pre-assembly

Prior to initiation of FLS collagen assembly, the precipitating solution consists of acidified calf-skin type I collagen and bovine serum-derived α_1 -acid glycoprotein. AFM images of the precipitating solution cast on mica demonstrate a relatively featureless film (Fig. 2b) with very occasional presence of filamentous materials (Fig. 2a). In a typical diluted sample, the entire surface where the aliquot droplet was deposited was covered with protein film and filamentous materials were observed very rarely, in much less than 5% of the samples scanned by AFM. This is difficult to estimate with certainty, since we are explicitly looking for these features which differ from the background film. Diameters of these filaments are estimated at 3–7 nm (exact measurements were difficult due to the typical embedding of the microfibrils in the background protein film) and lengths are on the order of a few microns. As with the following fibrillar structures, the features and morphologies of these microfibrils were consistent between aliquots taken in multiple fibrillogenesis experiments. These images are indistinguishable from those observed for acidic collagen solution without the added α_1 -acid glycoprotein. From a morphological perspective, the filamentous materials found in these pre-assembly solutions resemble the long, flexible microfibrils that dominate the early stages of the assembly of native-type collagen, as we have previously observed by AFM (Gale et al., 1995; Goh et al., 1997). They are presumably remnants of the original collagenous material, which were not solubilized completely into monomers by the acidification process in the preparation of the stock solution and which were not removed by the subsequent centrifugation and filtration steps: while almost all such materials are removed during these steps, a few rare fibrils may have remained.

Although there is some controversy in the literature over the effects of already assembled impurities in such redissolved collagen extracts (e.g. Holmes et al., 2001), we are readily able to form segmental long spacing collagen, which is composed of monomers packed in an unstaggered two-dimensional crystallite, from collagen stock solutions produced with the same protocol (Paige and Goh, 2001; Rainey and Goh, 2002). Under the acidic (pH 3.5–3.8) conditions employed in these previous studies, crystallites of one monomer in length were observed almost exclusively. Well below 1% of the crystallites were seen in dimer or trimer end-on-end aggregates, and no polymeric end-on-end SLS was

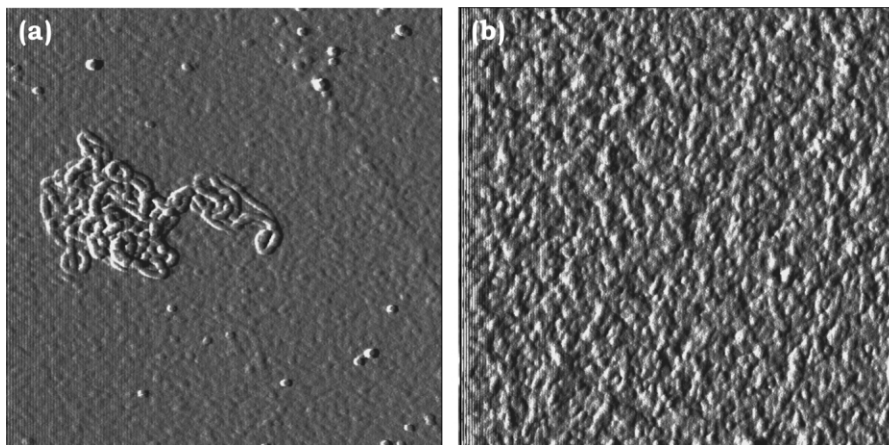


Fig. 2. Acidified pre-dialysis precipitating solution containing type I collagen and α_1 -acid glycoprotein. Contact mode AFM deflection images: (a) microfibrillar clump ($4 \times 4 \mu\text{m}^2$); (b) typical protein film on mica substrate, as in background of (a) ($2 \times 2 \mu\text{m}^2$).

observed. Therefore, we believe that these collagen stock solutions are composed of significant numbers of collagen monomers and small, reversibly associated oligomers; otherwise, formation of these crystallites would not be readily possible or preferred. Following this evidence of readily available monomer units, we do not believe that the presence of microfibril impurities in the initial solution is essential for the assembly—e.g. to serve as the sole nucleation sites in the assembly solution, since we are readily able to form large numbers of morphologically indistinguishable assembly products independent of the numbers of such aggregates observed. However, if a substantial number of these are present, they would likely affect the assembly, and we thus make an effort to minimize their presence.

2.2. Light scattering and pH measurements

During dialysis of the precipitating solution of α_1 -acid glycoprotein and collagen against deionized water, the pH changes slowly from an initial value of ~ 3.5 to final value of ~ 5.5 . This is accompanied by a marked increase in turbidity of the solution. The intensity of scattered light increases with increasing pH in a nonlinear S-shaped fashion: slower at low pH, and faster beyond $\sim \text{pH } 4$. The following discussion will thus be divided into three regimes—low pH (below $\sim \text{pH } 4$), intermediate pH ($\sim \text{pH } 4$ to $\sim \text{pH } 4.6$), and high pH (above $\sim \text{pH } 4.6$)—which later will be seen to have marked differences in the solution contents. Note that because of the discrete nature of the sampling, we cannot pinpoint transition regions very accurately. Furthermore, the rate of pH increase caused by the dialysis is somewhat different in every solution. Therefore, we do not attempt any quantitative analysis at this point; instead, we primarily use the scattering intensity in conjunction with pH measurements to provide a second,

independent indicator of fibrillogenesis events. This allows prudent choice of the most consistent aliquots for AFM imaging purposes. In general, an increase in the number of scattering units, as well as any increase in the diameter convoluted by the effect of increasing length dimensions of scattering units will lead to an increase in scattering intensity. Note that while scattering has been observed to be attenuated by increasing length of rigid rods (Doty and Steiner, 1950), the growing collagenous materials should be somewhat flexible and, therefore, not affect the light scattering in as straightforward a manner. For example, Deike et al. (2000) showed that static light scattering *increases* as a function of increasing molecular weight for stretched and aligned polyelectrolytes in an electric field. Therefore, while the majority of the scattering probably arises from diameter increase, we cannot predict the exact effect of increase in fibrillar length on the scattering intensity. By using AFM imaging alongside measured scattering intensity to investigate the constituents of the solutions during the fibrillogenesis process, we are able to observe the evolution of morphology that leads to the formation of mature FLS collagen.

2.3. Stages of the assembly

2.3.1. Early stage: below $\sim \text{pH } 4$

During this earliest dialysis stage, which takes approximately 2–6 h under our conditions, curly microfibrils appear more and more prevalent relative to the nondescript background protein film. By the end of the period, at least 80% of AFM scan areas contained these clumps and images were dominated by their appearance, as can be seen in Fig. 3. The very isolated clump in Fig. 2a as opposed to the much larger collection in Fig. 3a are typical of AFM scan features seen in the pre-dialysis mixture and towards the end of the early stage, respec-

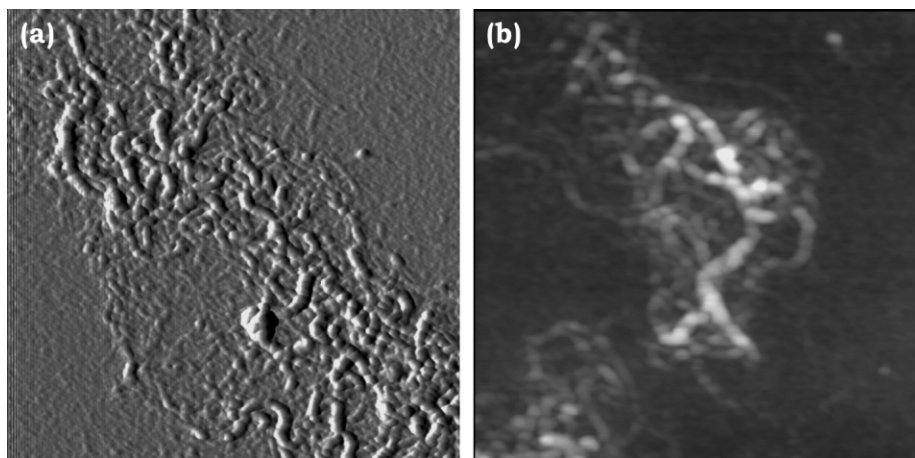


Fig. 3. Dialyzing FLS collagen solution in early stage of fibrillogenesis at pH 3.66. Contact mode AFM images demonstrating curly microfibril structures with no resolved banding: (a) deflection image ($3 \times 3 \mu\text{m}^2$); (b) height image ($2 \times 2 \mu\text{m}^2$; black: 0 nm, white: 30 nm).

tively. Beyond the increased numbers and, therefore, clumping, these microfibrils are morphologically indistinguishable. (Quantitative analysis of microfibrillar ultrastructure is still not readily possible at the imaging concentrations employed due to the intertangled nature of the fibrils and the microfibril embedding within the background protein film; general fibril dimensions are the same, at 3–7 nm in diameter and lengths on the order of a few microns.) The observation of such greatly increased numbers of indistinguishable microfibril structures supports the hypothesis that their presence in the stock solution is not essential for nucleation, although this cannot be proven unequivocally without the use of a purely monomeric stock solution. We can attribute the increase in light scattering intensity at this point to the increased numbers of these aggregates, which would scatter light due to both their increased length and diameter relative to the smaller α_1 -acid glycoprotein and collagen monomers and oligomers in the stock solution.

2.3.2. Intermediate stage: from \sim pH 4.0 to \sim 4.6

During this intermediate stage in FLS collagen fibrillogenesis, which occurs typically from 5 to 12 h of dialysis with our dialysis conditions, a different fibrillar morphology appears. When the dialysis solutions reach \sim pH 4, AFM images reveal the presence of thin fibrillar structures, some of which show banding with periodicity of \sim 270 nm. Examples of these structures are shown in Fig. 4a–d. This banding pattern matches that of the mature FLS fibril. The inset longitudinal-sections in Fig. 4b–d, with the dotted lines separated by exactly 135 nm serving as an aid to the eye, demonstrate that the banding is due to protrusions on the protofibril surface, which are approximately 2–3 nm higher than the interband region. During this stage of the assembly, fibril diameters and lengths are approximately 3–12 nm, and approximately 3–20 μm , respectively. As the pH

increases, the diameters of these filaments generally increase.

Previous work on FLS collagen (Paige et al., 1998) noted the presence of protofibrils, which were then proposed as possible intermediates to the assembly. The fibrils we observe in this stage of the assembly are similar in dimensions to those protofibrils; beyond this dimensional similarity, the intermediate structures below demonstrate that these thin banded fibrils are likely the same species as the earlier protofibrils. Banding was not seen in those protofibrils, but this could be due to a lack of resolution. The thin, \sim 270 nm banded fibrils will be called protofibrils from here on.

As the dialysis proceeds further (i.e. with increasing time and pH), larger fibrillar aggregates with clear banding patterns are observed (Fig. 5a–d). These fibrils have similarities to mature FLS collagen fibrils as reported in the literature (Paige et al., 1998, 2001) and shown in Fig. 6, in terms of the banding and length, as well as in the presence of ultrastructure that can be attributed to protofibrils. Compared to mature fibrils, the fibrils found in this assembly stage appear to consist of much more loosely bound protofibrils and/or microfibrils, such that the deposition onto mica for AFM imaging flattens them considerably. Collagen fibrils, in general, interact strongly with mica. Hence, collagenous aggregates typically appear flattened by the deposition, well beyond accounting for tip convolution effects. However, the structures observed here are flattened extremely, as can be seen in Fig. 5a–c. The interaction with mica also serves to accentuate the protofibrils. These laterally aggregated structures will be referred to as intermediate fibrils, to distinguish them from the other fibrillar forms.

As the assembly progresses, the packing of the protofibrils tightens and they appear less flattened on the substrate in the intermediate fibrils, as can be seen in

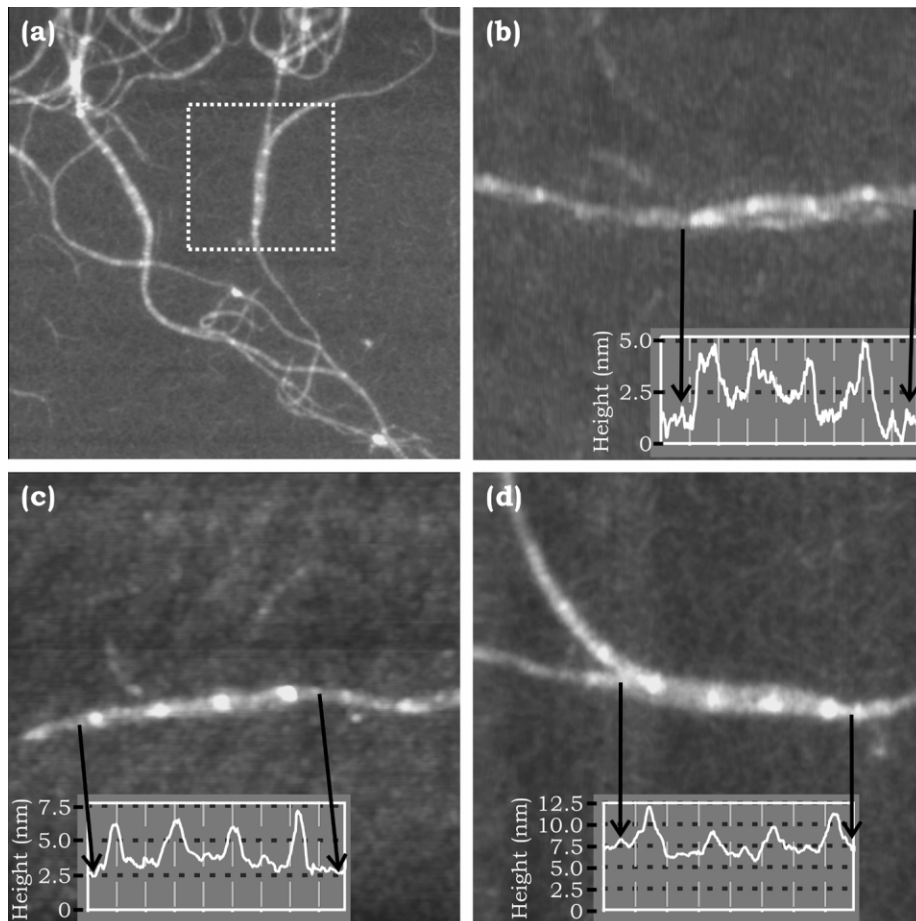


Fig. 4. Protofibril structures observed during the early intermediate stage of FLS collagen fibrillogenesis. Contact mode AFM height images (black: 0 nm height): (a) typical clusters of protofibrils at pH 4.25 ($5 \times 5 \mu\text{m}^2$; white: 35 nm); (b)–(d) $2 \times 2 \mu\text{m}^2$: (b) protofibril at pH 4 (white: 15 nm); (c) protofibril at pH 4 (white: 10 nm); and (d) 90° rotated zoom of boxed region in (a) (white: 30 nm). Insets in (b)–(d): longitudinal sections along indicated portion of fibril—the vertical lines are separated by 135 nm $\sim \frac{1}{2}$ the FLS collagen banding period.

Fig. 5d for a sample taken at pH 4.25. The diameters are now ~ 10 – 20 nm. From the AFM images obtained in this stage of the assembly, it appears that the protofibrils formed during the early stages associate laterally, in a manner such that their surface protrusions are in register, to form the intermediate fibrils. Branching is also often evident as the intermediate fibrils continue to associate, as can be seen throughout Fig. 5. The fact that banding periodicity is maintained in register at fibrillar branches is readily apparent, further demonstrating the alignment of protrusions in the constituent protofibrils.

Based on the AFM images, protofibrils and intermediate fibrils appear to be less flexible than the microfibrils that were found at low pH, probably due to their larger diameter-to-length ratio. The more rapid increase in turbidity at this stage of the assembly may be attributed most directly to the increased diameter and number of these less flexible fibrillar structures. The assembly steps observed in the current work, wherein

protofibrils with periodic protrusions associate laterally, is fully consistent with our previous observations of the existence of protofibrillar structures within the mature fibrils (Paige et al., 1998). The present study, though, provides a greatly improved ability to discern the intermediate structures and to allow speculation on their composition.

2.3.3. Late stage: above \sim pH 4.6

When the dialysis solutions reach \sim pH 4.6, typically between 10 and 18 h after initiating the dialysis, mature FLS fibrils that look similar to those previously observed by both AFM and EM begin to show up (Fig. 6). These are characterized by the existence of a clear banding period of ~ 270 nm, diameters of tens to hundreds of nanometers, and lengths of a few microns. Protofibrils are evident within the mature fibrils; fibrillar material is also evident on the surrounding substrate, but since we do not typically see banding, this is probably microfibrillar in nature. Unlike intermediate fibrils, the mature

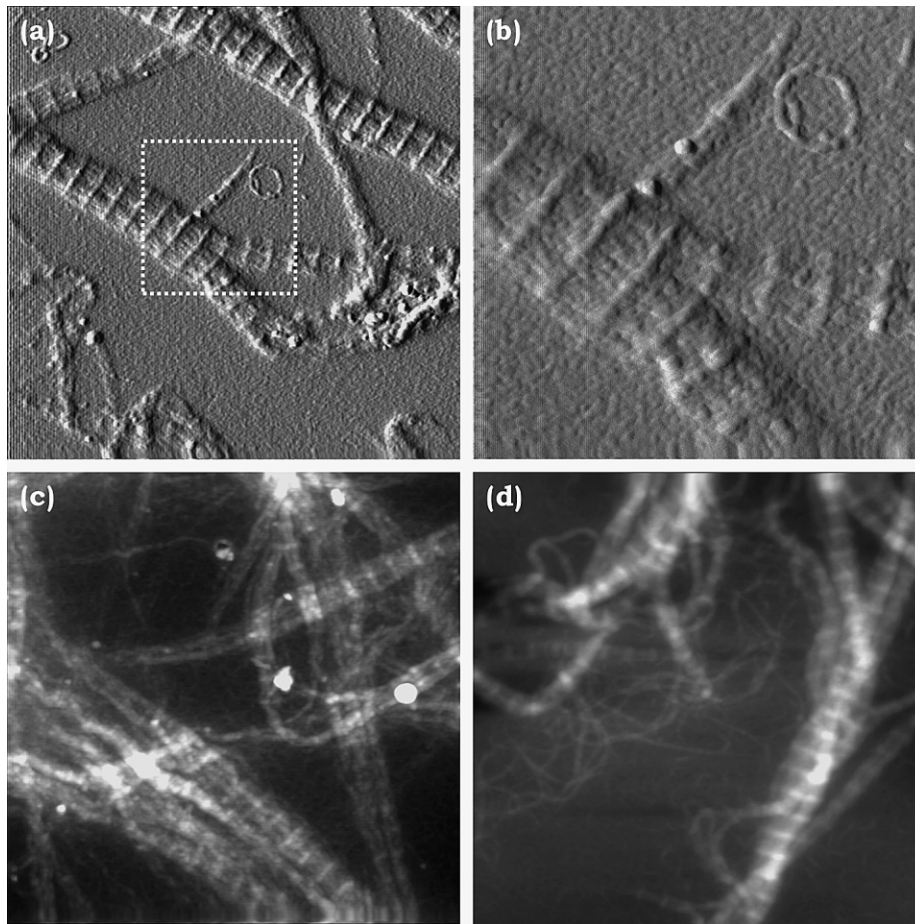


Fig. 5. Structures observed during late intermediate stage of FLS collagen fibrillogenesis. Contact mode AFM deflection images: (a) relatively loosely associated intermediate fibrils at pH 4.25 ($5 \times 5 \mu\text{m}^2$); (b) zoom in boxed region of (a) demonstrating protofibrillar constitution of intermediate fibrils ($2 \times 2 \mu\text{m}^2$); and, height images (black: 0 nm height): (c) intermediate fibrils demonstrating loosely associated protofibrils at pH 4.25 ($5 \times 5 \mu\text{m}^2$; white: 40 nm) and, (d) showing tightly associated protofibrils at pH 4.40 ($5 \times 5 \mu\text{m}^2$; white: 75 nm).

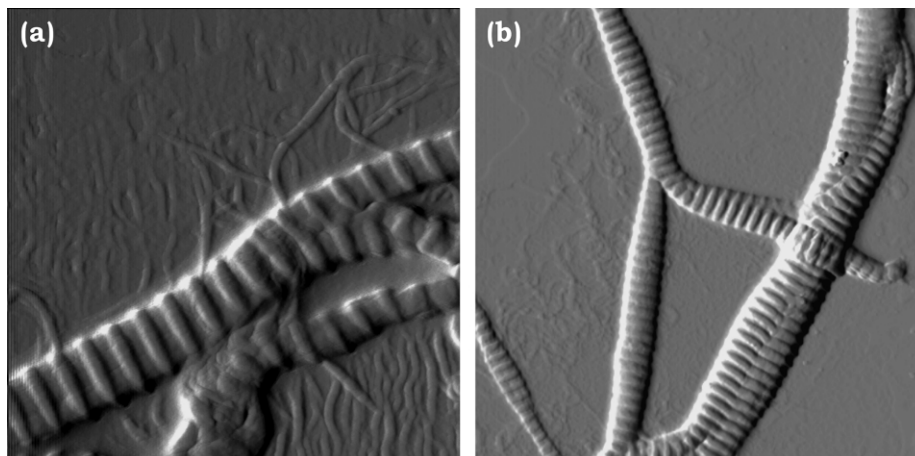


Fig. 6. Structures observed during fibril maturation stage of FLS collagen fibrillogenesis. Contact mode AFM deflection images: typical later growth stage fibrils observed at pH 4.59 (a: $2 \times 2 \mu\text{m}^2$) (b) and at pH 4.9 (b: $10 \times 10 \mu\text{m}^2$).

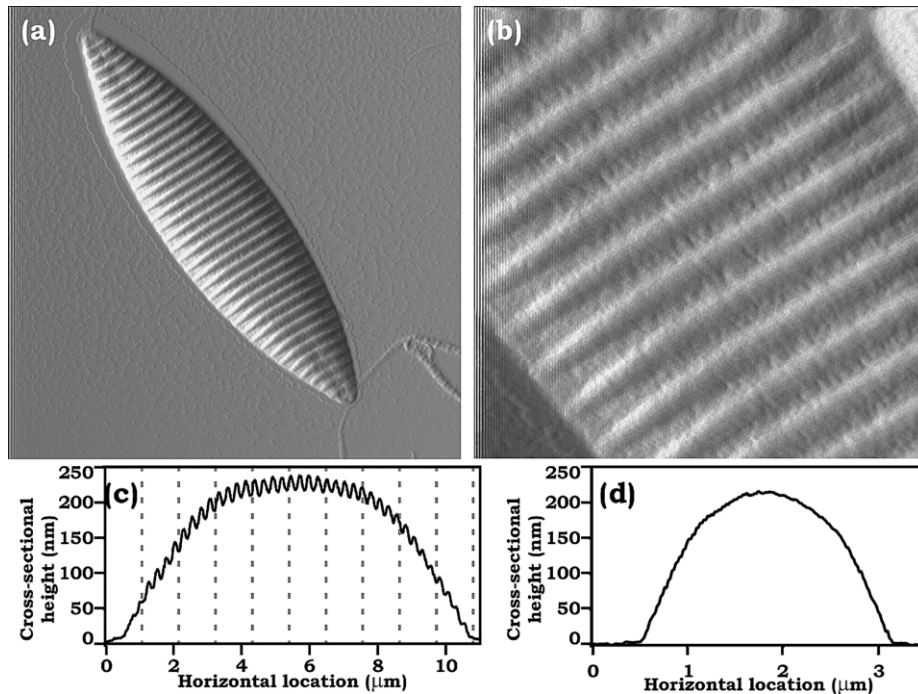


Fig. 7. Cocoon-like apparent assembly end-product observed after dialysis to pH 4.8. Contact mode AFM deflection images (a) $10 \times 10 \mu\text{m}^2$; (b) $1.5 \times 1.5 \mu\text{m}^2$ zoom in middle region of fibril shown in (a). (c) Longitudinal section along entire length of fibril shown in (a)—the dotted lines are spaced at 1080 nm, $\sim 4 \times$ the banding period of the FLS fibril. (d) Cross-section perpendicular to fibrillar long axis near middle of fibril. Note the different horizontal scales in (d) and (e).

fibrils appear much more compact, as can be seen by a comparison of Figs. 5 and 6. The branching observed in intermediate fibrils also persists in mature fibrils and pointed tips are frequently observed, as can be seen in Fig. 6b. Blunted tips are also sometimes observed in FLS fibrils, as shown by Paige et al. (1998). Whether these are truly stable fibrillar tips, or only quasi-stable structures trapped by deposition on a mica surface remains to be seen.

After the dialysis has proceeded for more than 12 or more hours, and the solution has reached \sim pH 4.8 or higher, a new morphology appears. Fibrils that have the characteristic 270 nm banding, but that are cocoon-like structures, often with pointed tips, are found to coexist with regular FLS fibrils (Fig. 7). These cocoons are large, with nominal diameters ranging from 200 nm to $1 \mu\text{m}$, and lengths of 4–20 μm . Because the height is greatly compressed compared to the width on adsorption (e.g. Fig. 7d), these diameters, measured as the maximum height above the substrate, are probably greatly underestimating the actual diameter in solution. Unlike typical fibrils, which remain fairly uniform in diameter until almost at the pointed tips, the most ideal cocoon-like fibrils taper off in diameter from the maximum at their middle; these pointed tips are very similar to some reported native collagen tactoids (e.g. Leibovich and Weiss, 1970). Some of these fibrils, like typical FLS collagen fibrils, also display blunted tips. Cocoon-like

fibrils have not been reported previously in FLS collagen, and we have correspondingly found that their formation is somewhat sporadic. This implies that the formation of cocoon structures is probably induced by some as yet undetermined combination of factors during fibrillogenesis. Aside from the general shape, these cocoons have the same banding features and surface ultrastructure as other mature FLS collagen fibrils.

2.4. The onset of banding in FLS collagen

In the early stages of the assembly, at low pH, no banded fibrils were seen; the only fibrillar structures are long, flexible microfibrils. While we are not able to pinpoint the transition accurately, it appears that there is a critical pH, that once attained initiates the formation of a different type of fibril, referred to herein as protofibrils. These protofibrils appear less flexible than the microfibrils in that all the images we obtain indicate less bending. An ultrastructure composed of protrusions that are spaced by ~ 270 nm first appears on these protofibrils. The repeated observation of the direct alignment of the protrusions on protofibrils in intermediate fibrils (as in Fig. 5) and the lack of obvious protrusions in the flat interband regions of the mature FLS collagen fibrils (Figs. 6 and 7, and Paige et al., 1998, 2001) implies that the protrusions observed at these early stages are the direct precursor of the periodic banded

structures which have been so highly characteristic of mature FLS collagen fibrils ever since the very first observations over 50 years ago.

While it is possible that these periodic protrusions are a result of some complex association between assembly intermediates that we are unable to see in these experiments, we prefer to consider the simple hypothesis that they are due to the binding of α_1 -acid glycoprotein to specific sites on the collagen, whether in monomer, microfibril, or protofibril form. This is readily possible. The pI of α_1 -acid glycoprotein is reported as anywhere from 2.8 to 3.8 (Fournier et al., 2000) and its glycan chains are highly sialylated. Sialic acid should be highly anionic at any pH during the dialysis, since it has a pK_a of ~ 2.2 (Traving and Schauer, 1998). As shown by Franzblau et al. (1976), removal of the sialyl units from α_1 -acid glycoprotein prevents FLS collagen from forming, demonstrating the necessity of these highly anionic species in the fibrillogenesis process. α_1 -Acid glycoprotein is found in vivo with a variety of glycan chain configurations (Schmid, 1989). A solution phase small angle neutron scattering study by Perkins et al. (1985) showed two possible conformations for the glycoprotein, depending upon the glycan units present. In the case of tri- or tetra-antennary glycans, which have been reported to make up $\sim 90\%$ of the mixture in humans (Yoshima et al., 1981), a compact, rod-like structure ~ 7 – 8 nm in length and 3 nm in diameter is proposed. In the remaining 10% of the human mixture, the bi-antennary conformation, the glycan units are seen to be highly flexible and typically extended away from the protein surface in ionic solution. The former conformation may be assumed to be that which would typically be observed in solution, leaving the anionic sialylated glycan units exposed on the surface of the protein. These could readily bind to collagen, which contains many basic arginine and lysine residues (Fietzek and Kuhn, 1976) which would be cationic at any pH under consideration. If the α_1 -acid glycoprotein is binding at the exact periodicity of the banding protrusions observed, the 2–3 nm increase in height may be attributable to the ~ 3 nm diameter proposed for the glycoprotein. In order for an FLS collagen fibril to be composed of ~ 40 – 45% by weight α_1 -acid glycoprotein, or 6–8 glycoprotein molecules per collagen monomer (Franzblau et al., 1976), then multiple binding events must occur and must be prevalent. In the early, isolated protofibril stage shown in Fig. 4, however, this cannot be differentiated from a single binding event. Furthermore, direct identification of the chemical species in this case is unfortunately not within the capability of the AFM.

2.5. Proposed fibrillogenesis pathway for FLS collagen

It would be best if we could observe the assembly in situ, but while AFM is potentially capable of such

studies, we have not yet been able to do so in this case. Instead, we sample the dialysis solution as a function of time, and attempt to reconstruct the assembly process based on the intermediate structures that are present at various times. There are distinct types of structures observed during the course of the assembly, the characteristics of which are summarized in Table 1: (i) at the start there are individual molecules, or small aggregates; (ii) long, flexible microfibrils that have no visible banding; (iii) thin, banded fibrils with periodic protrusions, which we designate as protofibrils; (iv) banded fibrils with loosely bound protofibrils, which we call intermediate fibrils; and (v) mature FLS fibrils, corresponding to previous FLS collagen studies. In some cases, the observed product is a large, cocoon-like structure instead of the somewhat narrower, typical fibrillar form. However, this may very well proceed via a different assembly pathway than normal FLS collagen. That such distinct morphology appears at different points in the assembly suggests that there is a stepwise nature to this process. Any assembly mechanism following this particular pathway, which is probably only one out of a competing ensemble, has to be consistent with the appearance of these observed intermediate structures, as well as the differentiation from native-type collagen assembly. Taking these considerations into account, our proposed assembly pathway is outlined in Fig. 8.

The first step (i in Fig. 8) is the formation of the long, flexible microfibrils, through the association of monomers and short oligomers. Similar microfibrils were found in native-type assembly (Gale et al., 1995; Goh et al., 1997), and this step may be the same for native-type and FLS collagen. Thus, α_1 -acid glycoprotein may not play a role in this process. However, it is also possible that α_1 -acid glycoprotein binds to some collagen monomers prior to their assembly into microfibrils and it is also quite likely that α_1 -acid glycoprotein affects the fibrillar assembly kinetics during this stage.

The next step (ii in Fig. 8) is the formation of protofibrils. As discussed in the previous section, we hypothesize that this is where α_1 -acid glycoprotein plays an important role, by binding to specific sites on collagen within the microfibrils. The bound α_1 -acid glycoprotein molecules thus correspond to the protrusions in the protofibrils, which are spaced apart by approximately 270 nm. The viscosity increase that was observed by Franzblau et al. (1976) to be crucial in FLS formation most likely corresponds to the onset of observation of protofibrils; i.e. to step ii in Fig. 8 becoming favourable. Viscosity increase is concomitant with collagen oligomerization (Na, 1989), which correlates well to the dramatic increase in microfibrillar species observed prior to protofibril formation. However, the role of the pH change in proceeding from step i to step ii in Fig. 8 cannot be discounted as a key factor.

Table 1

Morphological features of collagenous species observed during indicated stage of dialysis induced FLS collagen self-assembly with α_1 -acid glycoprotein; figures are given for representative AFM images, where appropriate

Species	Observed during	Length	Diameter ^a (nm)	Banding
Type I collagen monomer (Nimni, 1988)	Not resolved herein	~280–300 nm	~1.5	N/A
Microfibril	Pre-dialysis (Fig. 2) and early stage (Fig. 3)	2–7 μm	3–7	Unresolved
Protofibril	Early intermediate stage (Fig. 4)	2–20 μm	6–10	Protrusions separated by 270 nm
Intermediate fibril	Later intermediate stage (Fig. 5)	4–20 μm	10–20	Aligned 270 nm protofibrillar protrusions
Mature fibril	Late stage (Fig. 6)	4–20 μm	50–400	270 nm periodicity protrusions separated by flat, interband regions
Cocoon-like mature fibril	Late stage—extended dialysis (Fig. 7)	4–20 μm	200–1000	270 nm periodicity protrusions separated by interband regions

^a Diameter measurements are quoted as maximum measured heights above the flat imaging substrate; this is likely an underestimate of the solution state diameter.

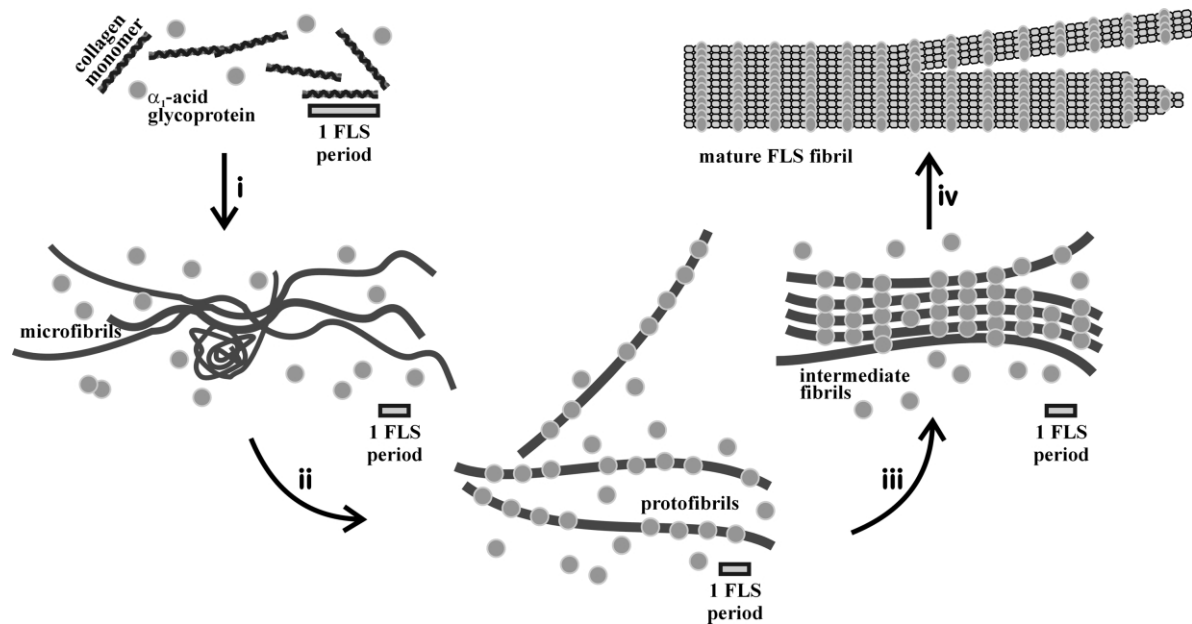


Fig. 8. Schematic of proposed assembly pathway for FLS collagen starting from collagen monomer/oligomer stock solution with α_1 -acid glycoprotein. (i) Microfibrils form from the collagen solution; these appear long and curly, typically in bunches, by AFM. (ii) α_1 -Acid glycoprotein adds to microfibrils (possibly in overlap region) forming protofibrils with protrusions at 270 nm periodicity; these are characteristically much less curved than microfibrils. (iii) Protofibrils, microfibrils and α_1 -acid glycoprotein self-assemble to intermediate fibrils. (iv) Continued assembly produces FLS collagen fibrils with protrusions spaced evenly at 270 nm. (These may be branched and may have pointed tips; tactoids are also sometimes observed.) Table 1 gives typical dimensions of structures observed by AFM. Note that the width and length dimensions are not to scale for the schematic; the relative scale of the FLS banding period is given for each stage prior to the final fibril.

The flexibility of these microfibrils implies a fairly short overlap period, allowing the typical flexibility observed in type I collagen monomers adsorbed to mica (Shattuck et al., 1994; Yamamoto et al., 2000) to be at least partially retained. Given the extensive literature on native collagen structure, the most likely molecular structure for these early stage microfibrils is a 4D-stagger (Kadler et al., 1996) in which each subsequent monomer overlaps at a stagger of 4D-periods as in Fig. 1b. This relates very well with the $\sim 0.4D$ overlapping fibrillar model determined to be most likely by Doyle et al. (1975), although the proposed anti-parallel lateral association cannot be tested here. From our present results, the degree and nature of lateral association in these intermediate assembly species is rather uncertain. However, lateral association must be taking place to some degree since the diameters of 3–7 nm for the flexible microfibril structures indicate that these structures are not simply monomers (~ 1 –2 nm diameter) associated by a 4D-stagger.

Whether binding of α_1 -acid glycoprotein to the fibrillar species serves to reduce fibril flexibility, or pH increase reduces fibrillar flexibility which then promotes α_1 -acid glycoprotein binding cannot yet be discerned. In either mechanism, the entropic disfavour of lateral association of the microfibrils would be decreased with

decreasing fibril flexibility. In addition, we can postulate that α_1 -acid glycoprotein, being a reasonably large polyanion, can serve to bind two fibrils together. Intermediate fibrils are thus formed (step iii in Fig. 8) when protofibrils encounter each other. One can imagine a zipper-like mechanism, where the association is initiated at a few points where α_1 -acid glycoprotein are bound. Equally possibly, a second microfibril could join side-by-side with a protofibril, binding to the exposed α_1 -acid glycoprotein. Thus, in intermediate fibrils, one sees laterally associated protofibrils and microfibrils where the protrusions, ascribed to the presence of α_1 -acid glycoprotein, are in register. The direct alignment of protrusions becomes particularly obvious when fibrillar branching is observed (e.g. Fig. 5). The ~ 270 nm spacing period implies that the α_1 -acid glycoprotein is promoting direct lateral association of the 4D-staggered microfibrils without significant further staggering (i.e. themselves staggered by 0D).

The strong interaction between the component protofibrils and microfibrils, mediated by α_1 -acid glycoprotein, serve to tighten their packing, resulting in the more compact structure of the mature FLS fibrils (step iv in Fig. 8). Microfibrils, protofibrils and intermediate fibrils may then continue to add to these mature FLS fibrils, resulting in growth of diameter with time. α_1 -Acid

glycoprotein likely continues to bind as well, leading to the final fibril form which only contains one collagen molecule for every 6–8 α_1 -acid glycoproteins.

The exact molecular orientations and locations of individual collagen molecules in the FLS fibril can be predicted, as discussed above, but cannot yet be determined with certainty. We can rule out the simplest 0D-stagger fibrillar structure given in Fig. 1a, since a stagger of some nature is necessary to provide spacing clearly less than the monomer length. This seems most likely to be a coherent lateral association of 4D-staggered microfibril subunits bridged by α_1 -acid glycoprotein, leading to the ubiquitous banding at 252–270 nm (or ~90% of the 280–300 nm monomer length). Furthermore, lack of any stagger whatsoever is difficult to rationalize with the fairly clear involvement of α_1 -acid glycoprotein as a necessary building block beginning in the protofibril stage after the formation of microfibrils which are presumably 4D-staggered.

What is still missing in this picture is the detailed role of slow pH change in the assembly. At low pH (i.e. the starting pH of ~3.5), all the acidic amino acids are nearly neutral, while the basic amino acids are positively charged, resulting in a net positive charge to the collagen monomer. As the pH increases, some acidic amino acids get deprotonated, and the charge distribution is altered. This implies that the step-wise assembly is effected by the slow change in charge distribution, which enables events to occur sequentially. Understanding the nature of the charge distribution will be a key to extracting the details of the assembly, and we are currently working on this problem.

3. Conclusions

The mechanisms underlying the differential formation of various collagenous constructs, both *in vitro* and *in vivo*, are still not well understood. FLS collagen is a construct with dramatically larger dimensions and different surface morphology than the typical fibrillar form of native collagen. The major identifying feature of FLS collagen since its discovery in 1950 by Highberger et al. (1950) has been the clearly periodic spacing at 250–270 nm observable by both TEM and AFM. Beyond the necessity of a second species, in this case α_1 -acid glycoprotein, little is known about the reasons for preferential formation of FLS collagen over native collagen.

AFM imaging allowed the investigation of structures present during the course of dialysis to form FLS collagen allowed three apparently stable intermediates in the FLS collagen fibrillogenesis pathway to be shown, along with the precise identification of the onset of the long-spacing banding. Below a cut-off pH of ~4, no coherent banding is apparent on the thin, curly fibrillar structures seen. Once this pH is surpassed by dialysis,

protrusions begin to appear on the thin, curly fibrils at exactly the long-spacing banding periodicity of mature FLS collagen. These early protrusions have a strong predisposition towards lateral association, as demonstrated by AFM imaging of further intermediates in the assembly. Eventually, mature FLS collagen fibrils, as previously reported, become predominant. The proposed model is that of 4D-period staggered microfibril subunits assembled laterally with little further stagger. The role of α_1 -acid glycoprotein is presumably in driving this lateral assembly over the standard microfibrillar self-assembly to produce 1D-period native-type stagger. Cocoon-shaped fibrils microns in length and up to a micron in diameter may also be produced.

4. Experimental procedures

4.1. *In vitro* FLS collagen self-assembly

A ~1 mg/ml acidified collagen stock solution was prepared by the following procedure. Type I calf-skin collagen (~99% purity, Sigma, St. Louis, MO) was dissolved in a solution of 0.01 M acetic acid in deionized water with gentle shaking to a concentration of ~1 mg/ml. It was then allowed to dissolve overnight at 4 °C, producing a cloudy white solution. This was then centrifuged at 47 808×g for 60 min at 4 °C to remove remaining insoluble aggregates. After centrifugation, the clear supernatant was carefully decanted so as not to disturb the pellet, thus forming the ~1 mg/ml acidified collagen stock solution. A portion of this stock solution was filtered through a 0.45 μ m filters (Millex-HV, Millipore, Bedford, MA) before being combined with an equal volume of a 0.5 mg/ml α_1 -acid glycoprotein solution (~99% purity, bovine serum derived, Sigma), forming what is referred to as the precipitating solution. The α_1 -acid glycoprotein solution was prepared immediately prior to use by dissolving the white solid in an appropriate amount of 0.01 M HOAc solution at 4 °C. The precipitating solution containing ~0.5 mg/ml collagen and 0.25 mg/ml α_1 -acid glycoprotein was then transferred into soaked dialysis tubing with a molecular weight cut-off of 12–14 kDa (Spectra/Pro, Spectrum, Gardena, CA) and sealed. It then underwent dialysis against a water bath of deionized water at 21 °C. Typically, a total 8 ml volume of the precipitating mixture was dialyzed against 300 ml of water. The initial pH of a precipitating solution was ~3.5. After overnight dialysis, the pH increased to a level of ~5.5.

4.2. Sampling of the FLS collagen dialysis solution

Removing the dialysis tubing from the water bath over periodic 30 min intervals stopped the dialysis of the precipitating solution. During this time, pH and

scattered light intensity readings were quickly taken, and a 10 μ l aliquot was removed from the precipitating solution for AFM imaging. For pH and light scattering measurements, 2 ml of the precipitating solution was temporarily transferred from the dialysis tubing into a polystyrene cuvette. Upon completion of the measurements, which took approximately 5–10 min, this portion was quickly returned to the dialysis tubing and replaced in the water bath in order to continue dialysis. The dialysis was thus periodically interrupted in order to make light scattering and pH measurements, but since the final products were indistinguishable from those formed in an undisturbed FLS assembly, we assume that the disruption was relatively minimal, although the overall kinetics of the process are likely affected to some degree. The time scale of the interruptions was also purposely kept extremely short (5–10 min) relative to the overall dialysis period (upwards of 12 h). As a further note, collagen assembly may be continuing after deposition on mica. Given the strong adsorption of collagenous species to mica, which is not perturbed even after rehydration (for FLS collagen see Paige et al., 2002), we would not expect a lot of free collagen species to remain in solution upon deposition of the aliquot on mica. Therefore, during the \sim 10 min drying time (see below for details) we would not predict significant ongoing assembly; the more perturbing aspect would likely be the general and indiscriminate adsorption of all species to the mica substrate. (It is impossible to avoid this drying step in any microscopic examination, unless the fibrillogenesis can be carried out *in situ*.) The intensity of scattered light was measured at 90° to the incident beam using a He–Ne laser; all measurements are reported relative to the maximum absorption for a given plot.

4.3. Atomic force microscopy

Samples for AFM imaging were prepared by diluting the 10 μ l samples tenfold with deionized water. These were immediately deposited onto freshly cleaved mica surfaces, then air-dried at ambient temperature and pressure. Images were captured using a Nanoscope III (Digital Instruments, Santa Barbara, CA) operating in contact mode. Square pyramidal silicon nitride tips with spring constant \sim 0.58 N/m were used (Nanoprobe, Digital Instruments), and they were frequently changed in order to minimize tip artefacts. Fibril diameters, lengths and banding periodicities were measured by taking cross-sections of the respective images of the fibril in height mode. For diameter measurements, the maximum height of the fibril above the substrate was used in order to avoid the tip convolution (Chicon et al., 1987; Keller, 1991) inherent in width measurements. Typically, reported measurements of structural features were compiled by examination of at least 30 fibrils from

several different sampling areas obtained from several fibrillogenesis runs. In the discussion, longitudinal- and cross-sections refer to section (on a height mode image) taken parallel and perpendicular to the long axis of a fibrillar species, respectively.

We have opted to allow the samples to dry at ambient temperature and pressure to avoid the introduction of possible drying artefacts by application of a pressurized gas such as nitrogen; even at such conditions, the majority of the droplet will have evaporated in \sim 10 min. As noted, dilutions were carried in deionized water prior to AFM imaging. Our primary reason for use of deionized water is to avoid the introduction of additional salts to complicate images, as would be found in buffer solutions. Upon dilution, the samples were applied to mica within seconds in an attempt to minimize any adverse effects. Furthermore, while the images presented are typically of diluted samples, to provide more regions with a sample density low enough to allow examination of single collagenous species, we see the same structures in aliquots deposited without dilution, implying that dilution is not drastically changing the structures observed.

Acknowledgments

Funding for this work was provided by the Natural Sciences and Engineering Research Council of Canada (NSERC). JKR is grateful to NSERC for support in the form of a Postgraduate Scholarship. Thanks to Dr George Natchev for assistance in the set up of the static light scattering apparatus and to Alvin Lin for valuable discussions.

References

- Baselt, D.R., Revel, J.-P., Baldeschwieler, J.D., 1993. Subfibrillar structure of type I collagen observed by atomic force microscopy. *Biophys. J.* 65, 2644–2655.
- Bowen, W.R., Lovitt, R.W., Wright, C.J., 2000. Application of atomic force microscopy to the study of micromechanical properties of biological materials. *Biotechnol. Lett.* 22, 893–903.
- Chapman, J.A., Armitage, P.M., 1972. An analysis of fibrous long spacing forms of collagen. *Connect. Tissue Res.* 1, 31–37.
- Chapman, J.A., Tzaphlidou, M., Meek, K.M., Kadler, K.E., 1990. The collagen fibril—a model system for studying the staining and fixation of a protein. *Electron Microsc. Rev.* 3, 143–182.
- Chicon, R., Ortuno, M., Abellan, J., 1987. An algorithm for surface reconstruction in scanning tunneling microscopy. *Surf. Sci.* 181, 107–111.
- Christiansen, D.L., Huang, E.K., Silver, F.H., 2000. Assembly of type I collagen: fusion of fibril subunits and the influence of fibril diameter on mechanical properties. *Matrix Biol.* 19, 409–420.
- Comper, W.D., Veis, A., 1977a. Characterization of nuclei in *in vitro* collagen fibril formation. *Biopolymers* 16, 2133–2142.
- Comper, W.D., Veis, A., 1977b. The mechanism of nucleation for *in vitro* collagen fibril formation. *Biopolymers* 16, 2113–2131.
- Cox, R.W., Grant, R.A., Horne, R.W., 1967. The structure and assembly of collagen fibrils. I. Native-collagen fibrils and their formation from tropocollagen. *J. R. Microsc. Soc.* 87, 123–142.

- Deike, R.A., Martin, C., Weber, R., 2000. Electric field light scattering by flexible linear polyelectrolytes in aqueous solution. *Eur. Phys. J. E* 1, 195–202.
- Doty, P., Steiner, R.F., 1950. Light scattering and spectrophotometry of colloidal solutions. *J. Chem. Phys.* 18, 1211–1220.
- Doyle, B.B., Hukins, W.L., Hulmes, D.J.S., Miller, A., Woodhead-Galloway, J., 1975. Collagen polymorphism: its origins in the amino acid sequence. *J. Mol. Biol.* 91, 79–99.
- Eyden, B., Tzaphlidou, M., 2001. Structural variations of collagen in normal and pathological tissues: role of electron microscopy. *Micron* 32, 287–300.
- Fietzek, P.P., Kuhn, K., 1976. The primary structure of collagen. *Int. Rev. Connect. Tissue Res.* 7, 1–60.
- Fournier, T., Medjoubi, N.N., Porquet, D., 2000. Alpha-1-acid glycoprotein. *Biochim. Biophys. Acta* 1482, 157–171.
- Franzblau, C., Schmid, K., Faris, B., et al., 1976. The interaction of collagen with α_1 -acid glycoprotein. *Biochim. Biophys. Acta* 427, 302–314.
- Fujita, Y., Kobayashi, K., Hoshino, T., 1997. Atomic force microscopy of collagen molecules. Surface morphology of segment-long-spacing (SLS) crystallites of collagen. *J. Electron Microsc.* 46, 321–326.
- Gale, M., Pollanen, M.S., Markiewicz, P., Goh, M.C., 1995. Sequential assembly of collagen revealed by atomic force microscopy. *Biophys. J.* 68, 2124–2128.
- Gelman, R.A., Williams, B.R., Piez, K.A., 1979. Collagen fibril formation. Evidence for a multistep process. *J. Biol. Chem.* 254, 180–186.
- Ghadially, F.N., 1988. *Ultrastructural Pathology of the Cell and Matrix*. Butterworths, London.
- Goh, M.C., Paige, M.F., Gale, M.A., Yadegari, I., Edirisinghe, M., Strzelczyk, J., 1997. Fibril formation in collagen. *Physica A* 239, 95–102.
- Gross, J., Highberger, J.H., Schmitt, F.O., 1952. Some factors involved in the fibrogenesis of collagen in vitro. *Proc. Soc. Exp. Biol. Med.* 80, 462–465.
- Gross, J., Highberger, J.H., Schmitt, F.O., 1954. Collagen structures considered as states of aggregation of a kinetic unit. The tropocollagen particle. *Proc. Natl. Acad. Sci. USA* 40, 679–688.
- Highberger, J.F., Gross, J., Schmitt, F.O., 1950. Electron microscope observations of certain fibrous structures obtained from connective tissue extracts. *J. Am. Chem. Soc.* 72, 3321–3322.
- Highberger, J.H., Gross, J., Schmitt, F.O., 1951. The interaction of mucoprotein with soluble collagen; an electron microscope study. *Proc. Natl. Acad. Sci. USA* 37, 286–291.
- Holmes, D.F., Graham, H.K., Trotter, J.A., Kadler, K.E., 2001. STEM/TEM studies of collagen fibril assembly. *Micron* 32, 273–285.
- Jandt, K.D., Finke, M., Cacciafesta, P., 2000. Aspects of the physical chemistry of polymers, biomaterials and mineralised tissues investigated with atomic force microscopy (AFM). *Colloids Surf. B* 19, 301–314.
- Kadler, K.E., Holmes, D.F., Trotter, J.A., Chapman, J.A., 1996. Collagen fibril formation. *Biochem. J.* 316, 1–11.
- Keller, D., 1991. Reconstruction of STM and AFM images distorted by finite-size tips. *Surf. Sci.* 253, 353–364.
- Kiselyova, O.I., Yaminsky, I.V., 1999. Scanning probe microscopy of proteins and protein-membrane complexes. *Colloid J.* 61, 1–19.
- Kuhn, K., 1982. Segment-long-spacing crystallites, a powerful tool in collagen research. *Coll. Relat. Res.* 2, 61–80.
- Leibovich, S.J., Weiss, J.B., 1970. Electron microscope studies of the effects of endo- and exopeptidase digestion on tropocollagen. A novel concept of the role of terminal regions in fibrillogenesis. *Biochim. Biophys. Acta* 214, 445–454.
- Lin, A.C., Goh, M.C., 2002a. A novel sample holder allowing atomic force microscopy on transmission electron microscopy specimen grids: repetitive, direct correlation between AFM and TEM images. *J. Microsc.* 205, 205–208.
- Lin, A.C., Goh, M.C., 2002b. Investigating the ultrastructure of fibrous long spacing collagen by parallel atomic force and transmission electron microscopy. *Proteins* 49, 378–384.
- Lowther, D.A., Natarajan, M., 1972. The influence of glycoprotein on collagen fibril formation in the presence of chondroitin sulphate proteoglycan. *Biochem. J.* 127, 607–608.
- Na, G.C., 1989. Monomer and oligomer of type-I collagen-molecular-properties and fibril assembly. *Biochemistry* 28, 7161–7167.
- Na, G.C., Butz, L.J., Carroll, R.J., 1986. Mechanism of in vitro collagen fibril assembly. Kinetic and morphological studies. *J. Biol. Chem.* 261, 12290–12299.
- Nimni, M.E., 1988. *Collagen*. CRC Press, Boca Raton, FL.
- Paige, M.F., Goh, M.C., 2001. Ultrastructure and assembly of segmental long spacing (SLS) collagen studied by atomic force microscopy. *Micron* 32, 355–361.
- Paige, M.F., Lin, A.C., Goh, M.C., 2002. Real-time enzymatic biodegradation of collagen fibrils monitored by atomic force microscopy. *Int. Biodeter. Biodegr.* 50, 1–10.
- Paige, M.F., Rainey, J.K., Goh, M.C., 1998. Fibrous long spacing collagen ultrastructure elucidated by atomic force microscopy. *Biophys. J.* 74, 3211–3216.
- Paige, M.F., Rainey, J.K., Goh, M.C., 2001. A study of fibrous long spacing collagen ultrastructure and assembly by atomic force microscopy. *Micron* 32, 341–353.
- Perkins, S.J., Kerckaert, J.P., Loucheux-Lefebvre, M.H., 1985. The shapes of biantennary and tri/tetraantennary alpha 1 acid glycoprotein by small-angle neutron and X-ray scattering. *Eur. J. Biochem.* 147, 525–531.
- Rainey, J.K., Goh, M.C., 2002. Parallel atomic force microscopy and NMR spectroscopy to investigate self-assembled protein-nucleotide aggregates. *J. Phys. Chem. B* 106, 5553–5560.
- Revenko, I., Sommer, F., Minh, D.T., Garrone, R., Franc, J.M., 1994. Atomic force microscopy study of the collagen fibre structure. *Biol. Cell* 80, 67–69.
- Schmid, K., 1989. Human plasma alpha 1-acid glycoprotein-biochemical properties, the amino acid sequence and the structure of the carbohydrate moiety, variants and polymorphism. *Prog. Clin. Biol. Res.* 300, 7–22.
- Schmitt, F.O., Gross, J., Highberger, J.H., 1953. A new particle type in certain connective tissue extracts. *Proc. Natl. Acad. Sci. USA* 39, 459–470.
- Shattuck, M.B., Gustafsson, G.L., Fisher, K.A., et al., 1994. Monomeric collagen imaged by cryogenic force microscopy. *J. Microsc.* 174, RP1–RP2.
- Traving, C., Schauer, R., 1998. Structure, function and metabolism of sialic acids. *Cell. Mol. Life Sci.* 54, 1330–1349.
- Trelstad, R.L., 1982. Multistep assembly of type I collagen fibrils. *Cell* 28, 197–198.
- Trelstad, R.L., Hayashi, K., Gross, J., 1976. Collagen fibrillogenesis: intermediate aggregates and suprafibrillar order. *Proc. Natl. Acad. Sci. USA* 73, 4027–4031.
- Vanamee, P., Porter, K.R., 1951. Observations with the electron microscope on the solvation and reconstitution of collagen. *J. Exp. Med.* 94, 255–266.
- Wood, G.C., Keech, M.K., 1960. The formation of fibrils from collagen solutions. 1. The effect of experimental conditions: kinetic and electron-microscope studies. *Biochem. J.* 75, 588–598.
- Yamamoto, S., Nakamura, F., Hitomi, J., et al., 2000. Atomic force microscopy of intact and digested collagen molecules. *J. Electron Microsc.* 49, 423–427.
- Yoshima, H., Matsumoto, A., Mizuochi, T., Kawasaki, T., Kobata, A., 1981. Comparative study of the carbohydrate moieties of rat and human plasma alpha 1-acid glycoproteins. *J. Biol. Chem.* 256, 8476–8484.